Translesion synthesis mechanisms depend on the nature of DNA damage in UV-irradiated human cells

Annabel Quinet[1],*, Davi Jardim Martins[1], Alexandre Teixeira Vessoni[1], Denis Biard[2], Alain Sarasin[3], Anne Stary[3] and Carlos Frederico Martins Menck[1],*

[1]Institute of Biomedical Sciences, University of São Paulo, SP, 05508-000, Brazil, [2]CEA, IMETI, SEPIA, Team Cellular Engineering and Human Syndromes, F-92265 Fontenay-aux-Roses, France and [3]CNRS-UMR8200, Université Paris Sud, Institut de Cancérologie Gustave Roussy, 94805 Villejuif, France

ABSTRACT

Ultraviolet-induced 6-4 photoproducts (6-4PP) and cyclobutane pyrimidine dimers (CPD) can be tolerated by translesion DNA polymerases (TLS Pols) at stalled replication forks or by gap-filling. Here, we investigated the involvement of Polη, Rev1 and Rev3L (Polζ catalytic subunit) in the specific bypass of 6-4PP and CPD in repair-deficient XP-C human cells. We combined DNA fiber assay and novel methodologies for detection and quantification of single-stranded DNA (ssDNA) gaps on ongoing replication forks and postreplication repair (PRR) tracts in the human genome. We demonstrated that Rev3L, but not Rev1, is required for postreplicative gap-filling, while Polη and Rev1 are responsible for TLS at stalled replication forks. Moreover, specific photolyases were employed to show that in XP-C cells, CPD arrest replication forks, while 6-4PP are responsible for the generation of ssDNA gaps and PRR tracts. On the other hand, in the absence of Polη or Rev1, both types of lesion block replication forks progression. Altogether, the data directly show that, in the human genome, Polη and Rev1 bypass CPD and 6-4PP at replication forks, while only 6-4PP are also tolerated by a Polζ-dependent gap-filling mechanism, independent of S phase.

INTRODUCTION

Ultraviolet (UV) rays emitted by the sunlight are one of the most carcinogenic agents for humans. UV irradiation induces DNA damage, in particular pyrimidine dimers, that distort the DNA double helix, interfering with the progression of the replicative DNA polymerases (Pol) and leading to replicative stress (1). In humans, pyrimidine dimers are repaired by nucleotide excision repair (NER), and de-

fects in this pathway are the cause of genetic diseases, such as *Xeroderma Pigmentosum* (XP), characterized by a high frequency of tumors in sun-exposed skin (2,3). Short-wave UV irradiation causes essentially two types of DNA damage: cyclobutane pyrimidine dimers (CPD) and pyrimidine 6-4 pyrimidone (6-4PP) (4). Although 6-4PP are three to four times less frequent than CPD (5), they induce a much more pronounced distortion in the DNA molecule (6). Consequently, 6-4PP are completely repaired within 3–6 h upon UV exposure, while approximately 50% of CPD persist 24 h later (7).

There are two universal strategies to counteract replication fork arrest: template switch, or translesion DNA synthesis (TLS) (8). In TLS, specialized DNA Pols, such as Polη, Polι, Polκ, Rev1 and Polζ are recruited to damaged DNA and promote replication across the lesion (9). The most abundant UV-induced DNA damage, TT-CPD, is accurately bypassed by Polη alone (10), while the tolerance of highly distortive 6-4PP requires the action of two or more TLS Pols (11,12).

The two-polymerase TLS mechanism starts with the insertion of one or more nucleotides by an inserter Pol (Polη, Polι or Polκ), followed by the extension of the primer by an extender Pol (Polκ or Polζ) (11,13). Rev1 plays a noncatalytic role by mediating the recruitment of TLS Pols to the DNA clamp PCNA (Proliferating Cell Nuclear Antigen) (14,15). Both Rev1 and Polζ were shown to be involved in 6-4PP bypass (16–19). On the other hand, despite the ability of Polη to insert one nucleotide opposite to 6-4PP *in vitro* or in plasmid (20,21), it is not clear whether Polη plays a role in the bypass of this lesion in the genome (19,22).

TLS can occur by two non-mutually exclusive mechanisms: directly at stalled replication forks or by filling in single-stranded DNA (ssDNA) gaps (23,24). In the latter, replication forks are restarted downstream of the damage, and both the leading and the lagging strand are discontinuously replicated, with ssDNA gaps formed behind the advancing fork (25–27). These gaps are then repaired post-

---

*To whom correspondence should be addressed. Tel: +55 11 3091 7499; Email: annabel.quinet@gmail.com
Correspondence may also be addressed to Carlos Frederico Martins Menck. Tel: +55 11 3091 7499; Fax: +55 11 3091 7354; Email: cfmmenck@usp.br

replicatively by TLS Pols (26,27). However, how the choice is made between tolerance at the fork or through gap-filling is still currently unknown. Additionally, it is not clear in which pathway each TLS Pol is involved. For instance, Rev1 was shown to act not only at arrested replication forks (23) but also in G2 phase to fill in ssDNA gaps (28), as well as in both early and late pathways (18).

We have recently reported that in global-genome NER-deficient XP-C cells, UV-induced DNA damage is bypassed by both gap-filling pathway and directly at the stalled fork, while in XP-V cells, lesions were mainly stalled at the fork (24). As XP-V cells are NER-proficient, we hypothesized that the difference between these cell lines would be the persistence of 6-4PP in XP-C cells. Thus, in this work, our goal was to better characterize TLS mechanisms following UV-induced DNA damage and to evaluate how 6-4PP and CPD are specifically bypassed in the human genome. Because 6-4PP are rapidly removed, human XP-C fibroblasts were employed in this study to maximize the effects of this type of lesion. To evaluate the effects of only one of these two types of lesion, we used adenoviruses carrying CPD- or 6-4PP-photolyases, enzymes that have the ability to specifically repair CPD or 6-4PP in a light-dependent reaction (29). Moreover, we depleted Polη, Rev1 or the catalytic subunit of Polζ, Rev3L, in XP-C fibroblasts, and our study brings new insights into the cellular role of each of these TLS Pols in UV-induced DNA damage bypass in the human genome.

MATERIALS AND METHODS

Cell culture, establishment of cell lines and gene silencing

The SV40-transformed human fibroblasts XP4PA (XP-C cells), XP4PA corrected for *XPC* mutation (XP-C^{cor} cells) (24), XP12RO (XP-A cells) (30) and XP4PA cells depleted for TLS Pols were routinely cultured in DMEM (LGC, Cotia, Brazil) supplemented with 10% FBS (fetal bovine serum, Cultilab, Campinas, Brazil) and 1% penicillin/streptomycin (Invitrogen, Life Technologies, Carlsbad, CA, USA) in a humidified 5% CO$_2$ atmosphere at 37°C. The expression of *REV1* and *REV3L* was stably knocked down (KD) from XP4PA cells using lentiviral vectors carrying specific short-hairpin RNA (shRNA) from the Mission shRNA Library (Sigma-Aldrich, Saint Louis, MO, USA) as previously described (31). Briefly, lentivirus production was achieved by transfecting HEK293FT with Mission Lentiviral Packaging mix (Sigma-Aldrich) and the plasmid carrying the shRNA sequence of interest using linear PEI (Polyethylenimine, Polyscience, Warrington, PA, USA) as a transfection agent. Cell supernatants were collected 72 h after transfection, filtered-sterilized and concentrated by ultracentrifugation. Transduced cells were selected with 0.3 μg/ml of puromycin (Sigma-Aldrich) during 6 days. Cell populations depleted for Rev1 or Rev3L were used to avoid any secondary effect of lentiviral integration. See Supplementary Material for shRNA sequences. For better comparison among cell lines, the XP-C/Polη^{KD} cells (24) were also transduced with lentivirus carrying the shCT construct, hereafter referred as to XP-C shPolη cells. Transient KD were performed with siGenome SMART-pool (Dharmacon, Lafayette, CO, USA): Rev3L siRNA (M-006302-01) (32), Rev1 siRNA (M-008234-01) (33) and nontargeting siRNA Pool #1 (D-001206-13). Briefly, cells were transfected with 50 nM of siRNA using oligofectamine (Life Technologies), according to manufacturer's instructions, and cells were replated 48 h later for subsequent experiments.

Cell transduction of photolyases with recombinant adenovirus

Cells were transduced with recombinant adenovirus carrying cDNA coding either for a GFP-tagged CPD-photolyase (AdCPDphr), or for a GFP-tagged 6-4PP-photolyase (Ad6-4phr), as previously described (34). Briefly, 3×10^5 cells were plated in 35-mm dishes. The next day, the cells were washed with warm PBS and incubated for 30 min with 500 μl of PBS$^+$ (PBS supplemented with 890 μM CaCl$_2$ and 500 μM MgCl$_2$). Then, the cells were transduced with either adenovirus in 500 μl DMEM without serum or antibiotics for 1.5 h. Transduction was stopped by adding 1.5 ml of complete culture medium. The same procedure was performed without adenovirus for mock-transduced (control) cells. The next day, after evaluating GFP expression under a fluorescence microscope (as a readout for expression of photolyases), the cells were re-plated for subsequent experiments.

UVC irradiation, treatment with caffeine (CAF) and photoreactivation

Exponentially growing cells were washed with preheated PBS and exposed to a UVC lamp the day after plating. A VLX-3W radiometer was used to monitor UVC dose and the rates used were: 0.1 J/m^2/s^{-1} for low-dose UVC exposures and 0.75 J/m^2/s^{-1} for high UVC dose. Unirradiated cells were maintained without medium for the same time as their irradiated counterparts. Thereafter, fresh medium was added to the cells, and they were incubated for the indicated times. Photoreactivation was carried out immediately after UVC irradiation, in PBS$^+$ with the culture dishes placed on 0.2-cm thick glass, 10 cm above a circular fluorescent lamp (daylight lamp, Phillips, 15 W, emission 320–700 nm) for 1 h at room temperature. Afterward PBS$^+$ was discarded and fresh medium was added for subsequent incubation. For controls with no photoreactivation, culture dishes were wrapped in aluminum foil before being placed above the lamp. For concomitant treatment with caffeine (CAF, Sigma-Aldrich), after UVC exposure complete culture medium supplemented with 1 mM final concentration of CAF was added to the cells.

Quantitative RT-qPCR

Quantitative RT-qPCR was performed as described elsewhere (31). See Supplementary Material for more details and primers used.

Cell viability

Cell viability was assessed using the Cell Proliferation Kit II (XTT, Roche) as previously described (30). See Supplementary Material for more details. Cell viability is expressed as a percentage of the corresponding control.

Cell cycle and subG1 analyses

Both procedures were performed independently, described elsewhere (24) and are detailed in Supplementary Material. Briefly, for cell cycle analysis, cells were incubated with 10 μM bromodeoxyuridine (BrdU, Sigma-Aldrich) for 20 min prior to harvesting at 37°C. Replicating cells were stained with anti-BrdU (Dako, Glostrup, Denmark) and DNA content was stained with propidium iodide (PI) solution (20 μg/ml, 200 μg/ml RNase A (Invitrogen, Life Technologies), 0.1% Triton X-100). For SubG1 analysis, the supernatant with detached cells and attached cells were stained with PI solution (above). Samples were loaded on a Guava Flow Cytometer (Millipore, Billerica, MA, USA) and analyzed with CytoSoft Data Acquisition and Analysis Software (Millipore), and approximately 7000 events were acquired for cell cycle analyses and 10 000 cells were counted for SubG1 analyses.

ssDNA detection by modified neutral comet assay

The single-stranded DNA (ssDNA)-specific S1 endonuclease from *Aspergillus oryzae* (Invitrogen, Life Technologies) (35) was used to generate double-strand breaks (DSB) from UV-induced ssDNA sites (36). Lesions were resolved in a single gel electrophoresis assay (comet assay) as previously described (24) with modifications for the use of S1 nuclease. The comet slides were washed in S1 nuclease buffer (50 mM NaCl, 30 mM sodium acetate, pH 4.6 and 5% glycerol) before the addition of S1 nuclease (Invitrogen, Life Technologies) at 20 U/ml in 1× S1 nuclease buffer and 50 mM NaCl (supplied by the manufacturer) to half the slide for 30 min at 37°C. As a control, the other half of each slide was incubated with the same solution, but without the nuclease. See Supplementary Material for more details. Comets were stained with ethidium bromide, imaged with a fluorescence microscope (Olympus BX51, Olympus, Center Valley, PA, USA), and at least 50 comets were scored for each condition per slide with Kinetic Imaging Komet 6.0 (Andor ™ Technology, Belfast, UK). Independent experiments were performed four times in duplicate.

DNA fiber assay and detection of ssDNA gaps on ongoing forks with S1 nuclease

The progression of replication forks upon UV exposure was evaluated by a DNA fiber assay, with a 20-min pulse of chlorodeoxyuridine (CldU, Sigma-Aldrich) before UVC irradiation and a 60-min pulse of iododeoxyuridine (IdU) afterward (24). For experiments with cells expressing photolyases, upon UV irradiation, the cells were incubated with 200 μM IdU in PBS$^+$ supplemented with 5% FBS for 60 min at RT on the photoreactivation apparatus. For experiments with the ssDNA-specific S1 endonuclease, after an IdU pulse, the cells were treated with CSK100 buffer (100 mM NaCl, 300 mM sucrose, 3 mM MgCl$_2$, 10 mM MOPS, 0.5% Triton X-100) for 10 min at RT, then incubated with S1 nuclease buffer (50 mM NaCl, 30 mM sodium acetate pH 4.6, 10 mM zinc acetate and 5% glycerol) with or without S1 nuclease (Invitrogen, Life Technologies) at 20 U/ml for 30 min at 37°C. See Supplementary Material for more

details. DNA fibers were imaged using a fluorescent microscope (Axiovert 200, Zeiss, Jena, Germany) at a magnification of 1000×. Analyses were performed using Zeiss LSM Browser Software. All experiments were performed at least twice independently, and at least 100 fibers were counted for each slide. Results repeated in separate figures represent independent experiments.

Postreplication repair (PRR) tracts

PRR tract detection in human cells was adapted from Daigaku et al., who first performed the technique in budding yeast (27). Briefly, upon UV irradiation the cells received medium with 100 ng/ml of nocodazole (Sigma-Aldrich) for 24 h. For the last 4 h, 10 μM BrdU (Sigma-Aldrich) was added to the medium. Glass slides were prepared as for the DNA fiber assay (described above). ssDNA was stained with mouse anti-ssDNA antibody (Millipore) and anti-mouse Alexa Fluor 594, and BrdU was detected with rat anti-BrdU and anti-rat Alexa Fluor 488. The slides were mounted using Fluoroshield (Sigma-Aldrich) and DNA fibers were imaged using a fluorescent microscope (Axiovert 200, Zeiss) at a magnification of 1000×. Analyses were performed using Zeiss LSM Browser Software. All experiments were performed twice independently. For quantification, only ssDNA with no continuous BrdU staining and with at least one clear and distinguishable BrdU patch were evaluated. The lengths of ssDNA were converted into kilobases using the conversion factor 1 μm = 2.59 kb (27), and at least ten independent fibers were evaluated per condition and per experiment. Each figure represents different and independent experiments, performed simultaneously for proper comparison.

Statistical analysis

Statistical significance was assessed using Prism 5 (GraphPad Software Inc., San Diego, CA, USA) with the following tests: unpaired *t*-test, one-way ANOVA or two-way ANOVA followed by the Bonferroni test as specified in the figure captions.

RESULTS

Polη, Rev1 and Rev3L are crucial for XP-C cell survival upon low-dose UVC

UV-induced DNA lesions are repaired by NER and, more precisely, 6-4PP are completely removed within 3–6 h upon UV irradiation. To study the tolerance mechanisms of both CPD and 6-4PP, human global genome NER-deficient XP-C fibroblasts were employed in these experiments. XP-C cell lines stably depleted for the expression of *REV1* or the catalytic sub-unit of Polζ, *REV3L*, were established by short-hairpin RNA interference (shRNA), to further characterize the role of these TLS Pols in the bypass of UV-induced DNA damage. Gene silencing in those cells and in previously reported XP-C shPolη cells (24) was confirmed by quantitative RT-qPCR (Figure 1A). Importantly, *REV3L* is the only TLS Pol whose deletion causes embryonic lethality in mice and long-term depletion in human cells was
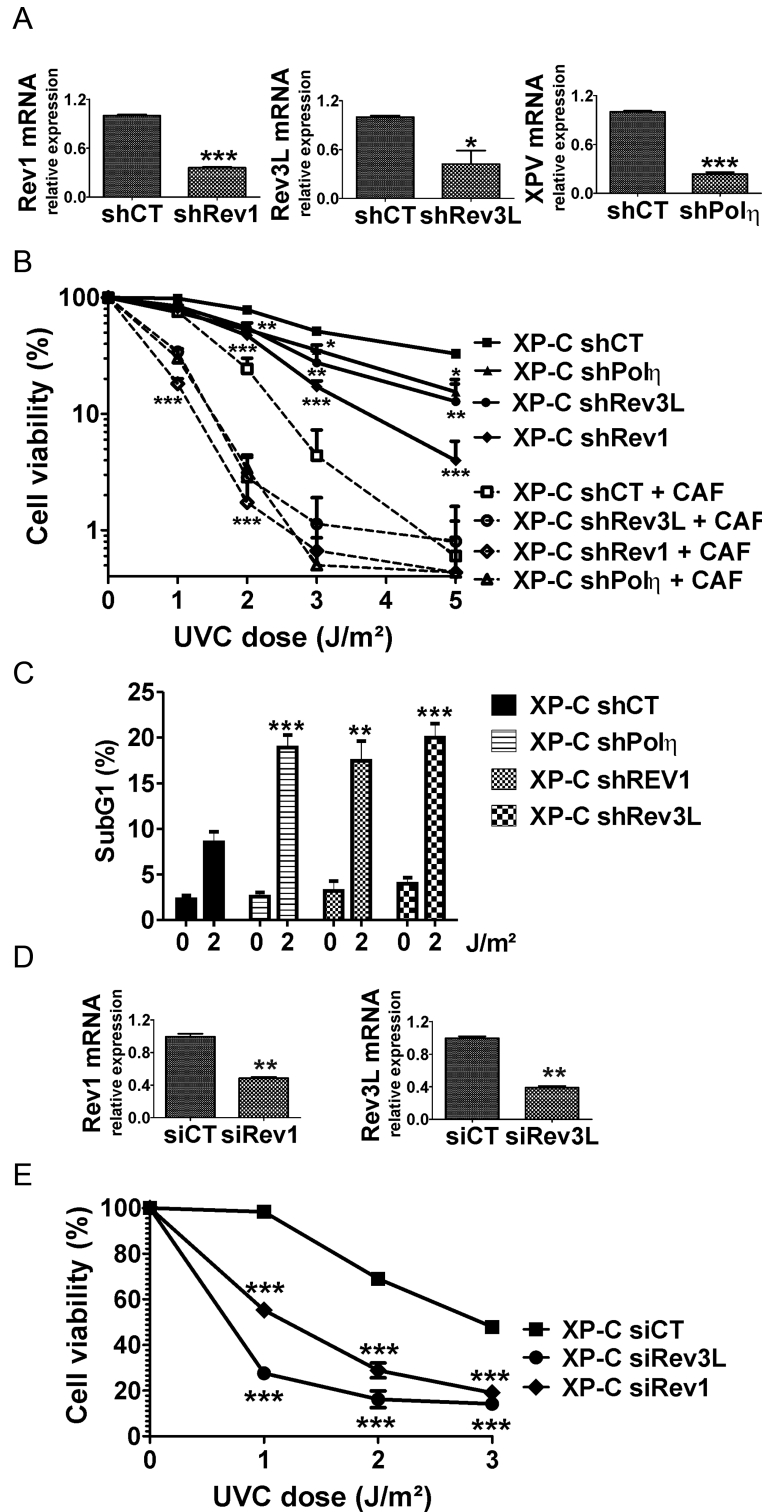
Figure 1. Depletion of Rev1, Rev3L or Polη sensitizes XP-C cells to low UVC-doses. (**A**) Validation of gene silencing with shRNA by RT-qPCR expressed as relative expression (means ± SEM) of control shRNA (shCT) (two independent experiments). Statistical significance was assessed by unpaired *t*-test. (**B**) Cell viability of XP-C shCT, XP-C shPolη, XP-C shRev1 and XP-C shRev3L was assessed 72 h after 1, 2, 3 or 5 J/m^2 UVC, with or without 1 mM caffeine (CAF) expressed as means (± SEM.) of percentages of nonirradiated control of three independent experiments. The statistical differences between depleted cells and control cells were assessed by one-way ANOVA followed by Bonferroni test. (**C**) SubG1 fraction 72 h after 2 J/m^2 expressed as average ± SEM from three independent experiments. The statistical differences between UV-exposed cells were assessed by one-way ANOVA followed by Bonferroni test. (**D**) Validation of gene silencing with siRNA by RT-qPCR expressed as relative expression. Statistical significance was assessed by unpaired *t*-test. (**E**) Cell viability of XP-C siCT, XP-C siRev1 and XP-C siRev3L 72 h after 1, 2 or 3 J/m^2 UVC expressed as means (± SEM) of percentages of control (two independent experiments). The statistical differences between depleted cells and control cells were assessed by one-way ANOVA followed by Bonferroni test. (* $P < 0.05$, ** $P < 0.01$, *** $P < 0.001$).

shown to cause the formation of micro-colonies that regained *REV3L* expression (32). In agreement, only XP-C cells with remaining expression of this gene were viable. Strikingly, despite this subsisting expression, the depletion of any of these Pols significantly sensitized XP-C cells to low-dose UVC irradiation, as assessed by cell viability (Figure 1B) and SubG1 population (Figure 1C) 72 h after irradiation. Interestingly, similarly to Polη depletion (24,37), Rev1 or Rev3L depletion significantly increased the toxicity of co-treatment with caffeine (CAF) and low-dose UVC in XP-C cells (Figure 1B). CAF has been associated with increased sensitivity to DNA damage in XP-V cells, due to the inhibition of ATM and ATR kinases (24,38,39). Thus, these results indicate that this increased sensitivity in the presence of CAF may be a more general phenomenon involving defective TLS, and not only Polη. In addition, transient gene silencing was performed in XP-C cells using a pool of siRNA targeting Rev1 (siRev1) or Rev3L (siRev3L). Gene silencing by siRNA were validated by RT-qPCR (Figure 1D) and also resulted in a significant increase in XP-C cell sensitivity to low UVC doses (Figure 1E). Altogether, these results functionally confirm the depletion of these Pols, and highlight that Polη, Rev1 and Rev3L are essential for XP-C cell survival upon low UVC dose exposure.

Rev1, but not Rev3L, depletion induces pronounced replication fork stalling in XP-C cells

Next, we analyzed the effect of low-dose UVC on the cell cycle distribution of Rev1- or Rev3L-depleted XP-C cells (Figure 2A and Supplementary Figure S1). Upon 2 J/m^2, XP-C cells expressing nontargeting shRNA (XP-C shCT) presented a temporary G2 phase arrest, while a higher UVC dose (5 J/m^2) induced a significant late S/G2 phase accumulation, as previously reported (24). To confirm these results, we knocked down *XPC* gene in MRC5 cells (NER-proficient fibroblasts) using siRNA (40) and observed similar late S/G2 phase arrest after UV irradiation (Supplementary Figure S1B). In XP-C cells, *REV1* or *REV3L* gene silencing did not affect the cell cycle distribution of nonirradiated cells (Figure 2A and Supplementary Figure S1A). Depletion of Rev1 led to an S phase arrest 24 h after exposure to 2 J/m^2 of UVC (from 45 to 54% of cells in the S phase) that was still significant 72 h later (54%). In these cells, 5 J/m^2 induced a strong arrest in the early S phase in 73% of cells, in a similar manner to the observed effect reported for XP-C shPolη cells (24). In XP-C shRev3L cells, exposure to 2 J/m^2 of UVC generated not only a temporary S phase arrest 24 h after treatment but also a significantly growing G2 phase accumulation of cells (14% of cells in G2 phase in the absence of irradiation, 22% at 24 h after 2 J/m^2 of UVC and 27% at 72 h). However, upon 5 J/m^2, XP-C shRev3L cells presented a strong accumulation of cells in the S phase. To confirm the impact of TLS Pols depletion in XP-C cells' replication, cell cycle was blocked in the G2 phase with the addition of nocodazole immediately after UV irradiation (Supplementary Figure S1C), avoiding the start of a new cell cycle, as previously described (41). As expected, all cell lines accumulated in the G2 phase in the absence of irradiation, however, upon 5 J/m^2, Polη- and Rev1-depleted cells showed a strong early S phase arrest, while most of XP-C

and XP-C shRev3L cells were arrested at late S/G2 phase. In addition, XP-C shRev1 and XP-C shRev3L clones were isolated, to check how varying degrees of gene silencing in cell populations could affect the results. Basically, clones silenced for each gene (Supplementary Figure S2A) are highly sensitive to low dose UV irradiation (Supplementary Figure S2B). Cell cycle analyses (in the absence or in the presence of nocodazole) of these clones also confirm that Rev1 depletion leads to a strong S phase arrest after UV irradiation, while shRev3L clones tend to have more cells reaching late S/G2 phase (Supplementary Figure S2C).

To better characterize the involvement of those TLS Pols in the progression of replication forks, we performed the DNA fiber assay. In this methodology, after a first pulse with one thymidine analog, chlorodeoxyuridine (CldU), cells are irradiated with 20 J/m^2 UVC, followed by a second pulse with another thymidine analog, iododeoxyuridine (IdU). We have recently shown (24) that irradiated XP-C cells exhibited a more pronounced replication fork stalling than their wild-type counterparts, only when a 20-min IdU pulse was performed. When a 60-min IdU pulse was applied, no more pronounced stalling of the replication forks was detected, suggesting that, at this time point, stalled forks have already been restarted in XP-C cells. Therefore, we repeated the 20–60 min setting on 20 J/m^2 (Figure 2B) in XP-C cells depleted for Rev1 or Rev3L using shRNA (Figure 2C) or siRNA (Figure 2D) and analyzed the CldU/IdU ratio. In the absence of irradiation, the expected CldU/IdU ratio should be 0.33 when a 60-min pulse of IdU is applied. In the presence of pyrimidine dimers in the genome, this ratio becomes higher because IdU length shortens due to the stalling of replication forks. Under these conditions, we observed that Rev1 depletion, with either shRNA or siRNA, significantly potentiated the effect of UV exposure on ongoing forks in XP-C cells. In contrast, *REV3L* gene silencing in XP-C cells, with both silencing strategies, had no significant effect on the progression of replication forks. Thus, Rev1, but not Rev3L, depletion results in clear fork stalling in UV irradiated cells. Significant effects of UV irradiation in CldU/IdU ratios in all cell lines corresponded to shorter IdU tracts (incorporated after UV exposure), while no effect was observed in the CldU tracts incorporated to nascent DNA before treatment (data not shown). This indicates that, at least in these experimental conditions, Rev1 and Rev3L are not involved in protecting nascent DNA from degradation upon UV irradiation, as observed by others for Rad51 after UV exposure (42) and Rev1 upon camptothecin treatment (43). Interestingly, without irradiation, XP-C cells depleted for Rev3L presented a slightly higher, although not statistically significant, CldU/IdU ratio than XP-C cells. It is noteworthy that Rev1 and in particular Rev3L depletion in XP-C cells led to shorter CldU track length in the absence of any treatment (Supplementary Figure S3), indicating that these Pols are required for progression of replication forks, even in the absence of exogenously induced DNA damage. Indeed, it was recently shown that Rev3L is essential for human cell proliferation (32).
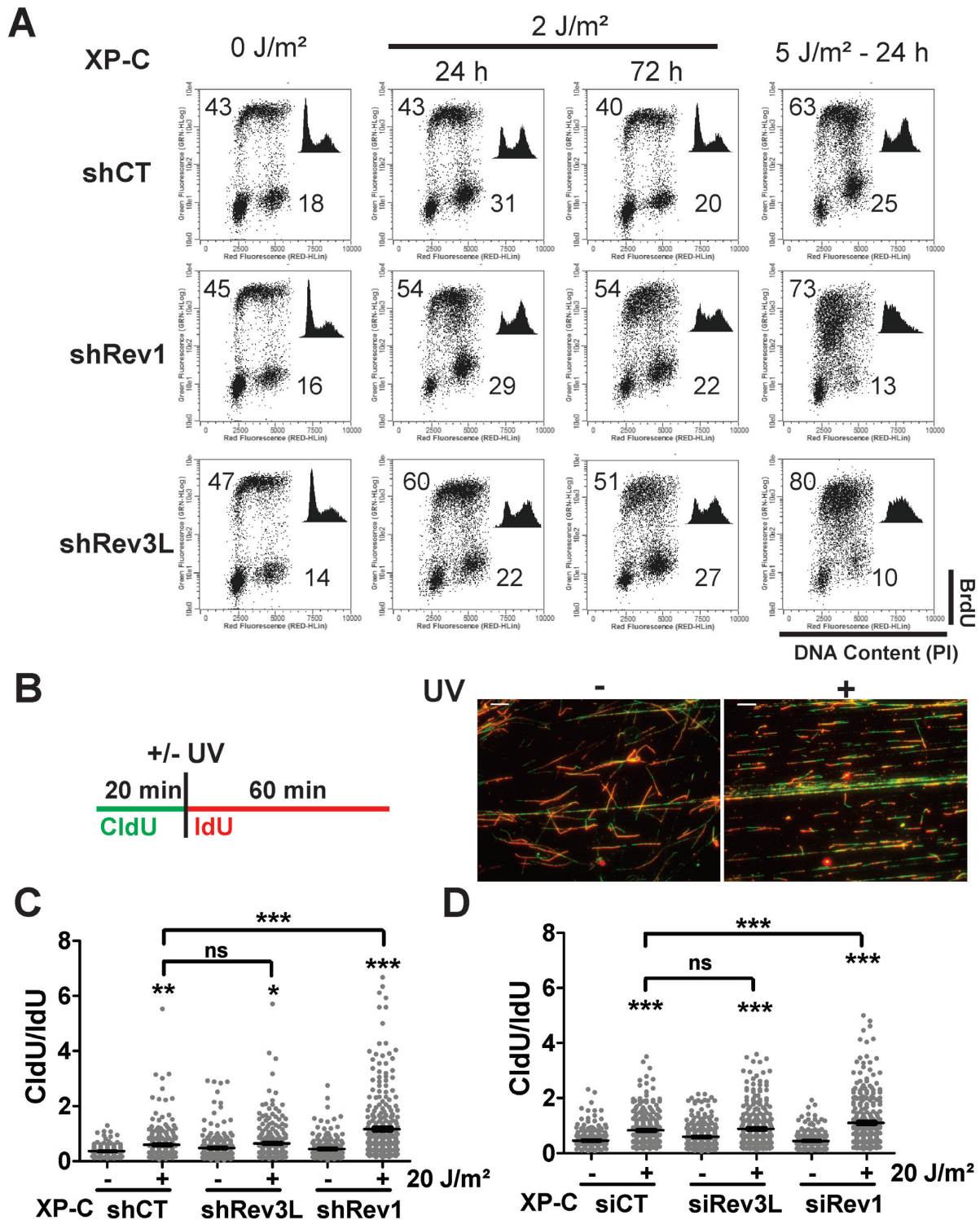
Figure 2. Effects of Rev1 or Rev3L depletion on XP-C cell cycle distribution and replication fork progression upon UV treatment. (**A**) Cell cycle phases of XP-C shCT, XP-C shRev1 and XP-C shRev3L were evaluated by BrdU and DNA content staining at the indicated times after UVC exposure. Graphics representative of three independent experiments are shown, and the averages of the percentages of cells in S and G2 phases are indicated. At the top right of each panel, the cell cycle distribution determined only by PI staining is shown. (**B**) Left. Scheme of DNA fiber assay performed with XP-C depleted for Rev1 or Rev3L upon 20 J/m^2 UVC. Right. Representative images of DNA fibers assessed with XPC siRev1 cells in the absence of treatment (−) or after 20 J/m^2 (+). The white bars correspond to 10 μM. CldU/IdU ratios from ≥100 fibers for 0 J/m^2, and ≥150 fibers for 20 J/m^2 of two independent experiments were scored for XP-C cells depleted for TLS Pols either with shRNA (**C**) or siRNA (**D**). Statistical significances were determined by one-way ANOVA followed by Bonferroni test (ns, non significant; * $P < 0.05$, ** $P < 0.01$, *** $P < 0.001$).

Rev3L depletion induces the accumulation of postreplicative ssDNA gaps in UV-exposed XP-C cells

Because Rev3L depletion in XP-C cells induced late UV-induced G2 phase accumulation of cells and did not affect replication fork progression upon UV exposure (Figure 2), we hypothesized that, in those cells, ssDNA gaps are generated from fork restart. Indeed, it has been reported that ssDNA gaps are inducers of checkpoint triggering G2 phase arrest (18,24,44). To address this question, we analyzed the formation of ssDNA regions in XP-C cells depleted for TLS Pols upon UV exposure. We performed a sensitive assay based on the ssDNA specificity of the S1 endonuclease from *Aspergillus oryzae* (35,36) followed by the detection of DNA double-strand breaks (DSB) generated by the neutral comet assay (Figure 3A and Supplementary Figure S4). First, in the absence of S1 nuclease, 24 h after UVC exposure, XP-C cells depleted for TLS Pols presented a significant dose-dependent increase of DSBs. This was particularly pronounced in XP-C cells depleted for Rev1. In XP-C shCT cells, a significant increase in the generation of DSBs was only observed upon a high UVC dose, 20 J/m^2 (Figure 3A and Supplementary Figure S4A). DSB formation in the absence of S1 nuclease may be due to fork collapse in the lack of TLS Pols and/or in the presence of high amounts of DNA damage, in agreement with previous reports (24,45,46). However, after addition of S1 nuclease, only XP-C shRev3L cells presented important dose-dependent increase in tail moment in UV-irradiated cells (Figure 3A and Supplementary Figure S4A). These data indicate that, in the absence of Rev3L, ssDNA regions accumulate in XP-C cells exposed to UVC. The effect of the S1 nuclease was even higher when XP-C shRev3L cells were arrested in the G2 phase with the addition of nocodazole upon 20 J/m^2 (Supplementary Figure S4A), indicating that ssDNA regions are mainly detected in this phase of the cell cycle. Under these conditions, we were still not able to detect any effect of S1 nuclease in XP-C cells (Supplementary Figure S4B), thus confirming that ssDNA regions do not accumulate in XP-C cells. In UV-exposed XP-C shPolη cells, we observed a slight effect of S1 nuclease, although significantly lower compared to XP-C shRev3L cells. Interestingly, in XP-C shRev1 cells, we did not detect statistically significant accumulation of ssDNA using this methodology (Figure 3A). Similar results, indicating the lack of ssDNA accumulation, were observed in a clone isolated from XP-C shRev1 cells population (Supplementary Figure S2) even after 20 J/m^2 with nocodazole (Supplementary Figure S4C). As previously suggested (24), we hypothesized that these ssDNA regions correspond to gaps generated from fork restart downstream the damage. Because DNA fiber assay does not allow the direct visualization of these gaps (45), we treated the nuclei with the S1 nuclease after the second pulse (IdU) and before spreading the DNA onto the glass (Figure 3B). If gaps were formed, ssDNA regions would be nicked by the nuclease, generating shorter IdU tracts. In XP-C^{cor} cells, addition of S1 nuclease had no effect in CldU/IdU ratio (Figure 3C). However, in both XP-C and XP-C shRev3L cells, the digestion by S1 nuclease significantly increased CldU/IdU ratio from UV-exposed cells and in a similar fashion (Figure 3D). On the other hand,
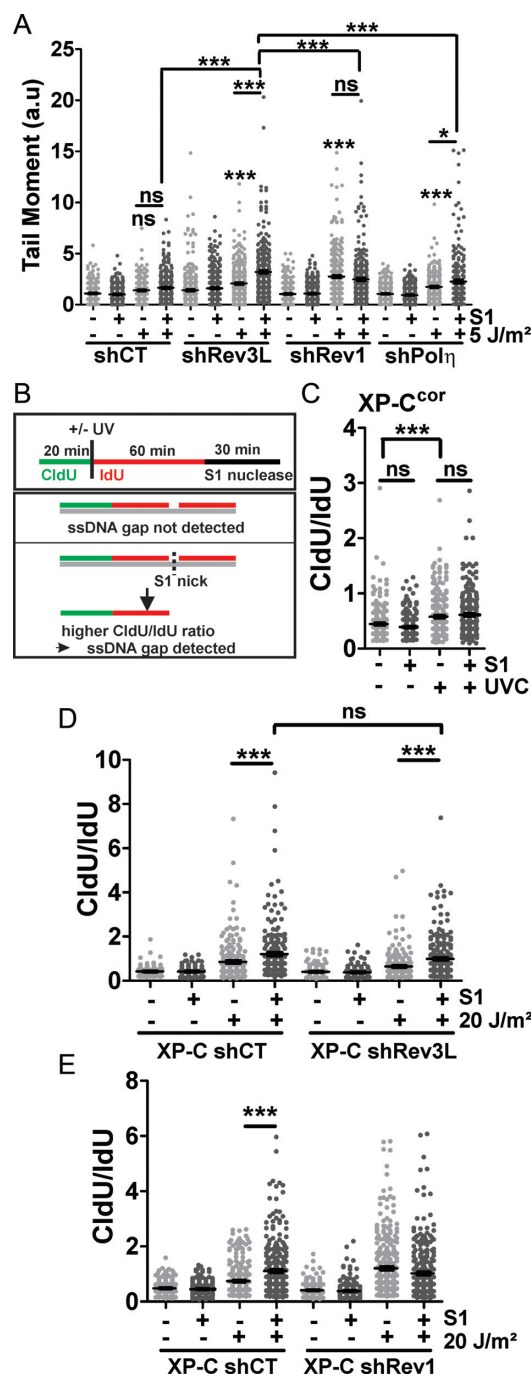

Figure 3. Detection of ssDNA gaps on ongoing replication forks. (**A**) Neutral comet assay with or without ssDNA-specific S1 endonuclease 24 h after 0 or 5 J/m^2 in XP-C cells depleted for TLS Pols with shRNA. Results are expressed as tail moment (average ± SEM) from ≥ 50 comets per condition of four independent experiments performed in duplicate. The significance of differences between UV-exposed cells compared to its respective untreated control, irradiated cells with or without S1, and between cell lines was assessed by one-way ANOVA followed by Bonferroni test. (**B**) Scheme of DNA fiber assay with the ssDNA-specific nuclease S1 for the detection of ssDNA gaps on ongoing forks. DNA fiber assay with or without S1 nuclease in XP-C^{cor} (**C**), XP-C shCT and XP-C shRev3L cells (**D**) and XP-C shCT and XP-C shRev1 (**E**) upon 0 or 20 J/m^2 UVC and represented by CldU/IdU ratios (average ± SEM) from two independent experiments each (≥100 fibers for 0 J/m^2 and ≥150 fibers for 20 J/m^2). Statistical significances were determined by one-way ANOVA followed by Bonferroni test (ns, non significant; * $P < 0.05$, ** $P < 0.01$, *** $P < 0.001$).

by comparing XP-C shCT and XP-C shRev1 cells (Figure 3E), we observed that in the latter, treatment with the S1 nuclease had no effect in CldU/IdU ratio in UV-exposed cells. Therefore, 1 h post UV treatment, ssDNA gaps were generated upon unrepaired DNA damage in XP-C cells independently of Rev3L, but not in Rev1-depleted cells. Because we were unable to detect ssDNA regions 24 h after UV in XP-C cells (Figure 3A and Supplementary Figure S4B), we hypothesized that at this time point, ssDNA gaps would have been repaired. To visualize and quantify postreplication repair (PRR) tracts in human cells, we adapted a procedure performed by Daigaku et al. in budding yeast (27) (Figure 4). In this sense, immediately after exposing XP-C cells to UVC, nocodazole was added to the medium for 24 h to avoid cells progression through mitosis (Supplementary Figure S5). During the last 4 h of nocodazole treatment, BrdU was added to the medium to be incorporated at the PRR tracts (Figure 4A and B), and BrdU patches (indicative of gap filling) were quantified upon immunostaining (Figure 4C–F). In UV-exposed XP-C cells, there was a significant increase in the amount of BrdU patches compared to mock-treated cells (Figure 4C) and this effect was dependent on the UVC dose (Supplementary Figure S6), in agreement with the report in budding yeast (27). The possibility that these BrdU patches are due to transcription-coupled repair DNA synthesis (functional in XP-C cells) was tested in XP-A (TCR and GGR NER-deficient) cells. The results reveal that XP-A cells also present a significant increase in BrdU patches density upon UV irradiation, similar to what was observed for XP-C cells (Figure 4D). In addition, NER-proficient XP-C^{cor} cells did not present any increase in the density of BrdU patches (Figure 4D). These results discard any participation of DNA repair and support the idea that BrdU patches correspond to PRR tracts. Upon 20 J/m^2 UVC, PRR tract density was 0.016 Kb^{-1}, which represents approximately 1 BrdU patch per 60 kb. By comparing XP-C cells depleted for TLS Pols with shRNA (Figure 4E) or with siRNA (Figure 4F), the depletion of Rev3L was the only one that resulted in the lack of increase in PRR tracts density upon UV. This is in agreement with the accumulation of ssDNA regions observed 24 h upon UV (Figure 3A and Supplementary Figure S4). Altogether, these data demonstrate that Rev3L is essential for PRR. Interestingly, PRR tracts density in XP-C depleted for Rev1 increased as in XP-C cells, after UV irradiation (Figure 4E and F), supporting the lack of accumulation of ssDNA regions shown in Figure 3A and Supplementary Figure S4C. However, we cannot exclude that the lack of effect in the gap-filling pathway in cells depleted for Polη or Rev1, are in fact due to incomplete knockdown. In summary, the results support that in XPC-deficient cells, replication forks are restarted leaving ssDNA regions. In XP-C cells and in XP-C cells depleted for Polη or Rev1, but not for Rev3L, these ssDNA gaps are repaired. As a consequence, ssDNA gap-filling in human cells is dependent on Polζ.

Photoremoval of CPD or 6-4PP has different effects in cell cycle distribution of UV-irradiated XP-C cells

To investigate whether the effects observed in XP-C cells are specifically due to 6-4PP or CPD, we employed a strategy based on cell transduction with recombinant adenovirus-carrying photolyases, as previously reported (34,47). These enzymes are able to specifically perform direct reversion of 6-4PP or CPD to monomers in a reaction that is dependent on visible light (29) (Supplementary Figure S7). Therefore, the consequences of only one type of UV-induced DNA damage in the human genome can be tracked. First, we evaluated the effect of specific photorepair on cell viability 72 h upon low-doses (2 or 3 J/m^2) of UVC (Supplementary Figure S8). We observed that both CPD- and 6-4PP photolyases protected XP-C and TLS Pols-deficient XP-C cell lines from low UVC doses. The specific repair of 6-4PP, rather than CPD, was highly protective against co-treatment with CAF and UVC (although not statistically significant for XP-C shRev3L cells). Importantly, in XP-V cells, which are NER-proficient but deficient for Polη, only the removal of CPD induced such protection. The protective effects of both photolyases were significantly reduced in the absence of light exposure. We next investigated the effects of specific 6-4PP or CPD photorepair in cell cycle distribution upon UV irradiation (Figure 5). In mock-transduced cells, results were comparable to those described above (Figure 2 and Supplementary Figure S1). Transduction with adenovirus did not induce any changes in the cell cycle profile in the absence of UV exposure (Figure 5B). Upon 2 and 5 J/m^2, the specific photoremoval of 6-4PPs significantly decreased the accumulation of XP-C cells in late S/G2 phase. This was also observed in XP-C cells depleted for TLS Pols 24 and 72 h after 2 J/m^2 (Figure 5B). Interestingly, 24 h upon 5 J/m^2, the specific photoremoval of 6-4PP resulted in a reduction in early S phase arrest in XP-C shRev1 and XP-C shPolη cells, resulting in more cells accumulated in late S/G2 phase. On the other hand, the photorepair of CPD did not have any significant effect on the cell cycle distribution of XP-C cells. However, in XP-C shPolη, XP-C shRev1 and XP-C shRev3L cells, CPD photoremoval reduced early S phase arrest (with accumulation of late S/G2 phase cells). In summary, 6-4PP photoremoval can attenuate the accumulation of cells in both early S and late S/G2 phases, while CPD repair leads to a strong reduction on cell arrest in the early S phase.

CPD, but not 6-4PP, photorepair attenuates replication fork stalling in XP-C cells, except when Polη or Rev1 is deficient

We also evaluated the involvement of 6-4PP or CPD in the stalling of replication forks observed in TLS Pols deficient XP-C cells (Figure 6). This question was addressed through the DNA fiber assay in which the 60-min IdU pulse was concomitant to photoreactivation (Figure 6A, see Materials and Methods section for further details). CldU/IdU ratio averages were not affected by adenoviral transduction, in untreated cells. However, since IdU incorporation under photoreactivation condition was slower (with CldU/IdU ratio averages approximately 0.9 in the absence of irradiation) (Figure 6B), cells were exposed to a higher UV dose (50 J/m^2) to enable the detection of significant replication fork arrest. Indeed, upon 50 J/m^2 mock-treated XP-C shCT cells presented significant replication fork stalling when compared to unirradiated cells. Depletion of Rev3L resulted in a similar effect, but fork stalling was significantly
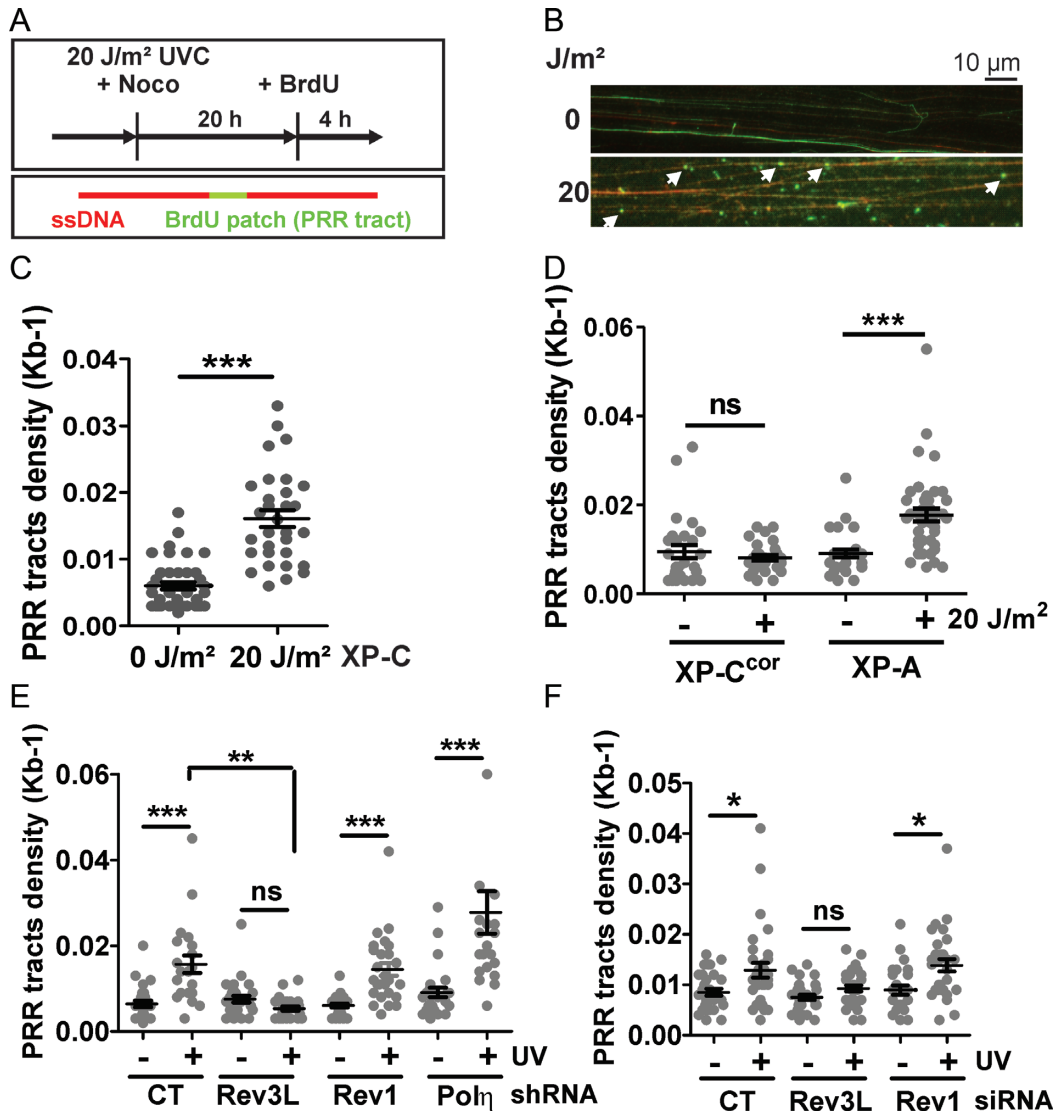
Figure 4. Detection of postreplication repair (PRR) tracts. (**A**) Experimental scheme for immunolabeling of PRR tracts. (**B**) Representative images of PRR tracts in XP-C shCT cells exposed to 0 (above) or 20 J/m² (below). The white arrows indicate BrdU patches (in green) that correspond to PRR tracts in ssDNA fiber (in red). Quantification of PRR tract density in XP-C shCT (**C**), in XP-C^{cor} and XP-A cells (**D**) and in XP-C cells depleted for TLS Pols either with shRNA (**E**) or siRNA (**F**) 24 h after 0 or 20 J/m². Results are represented as mean (± SEM) of PRR tracts density from two independent experiments each. The significance of differences was assessed by one-way ANOVA followed by Bonferroni test (ns, nonsignificant; * $P < 0.05$, ** $P < 0.01$, *** $P < 0.001$).

potentiated by Polη or Rev1 depletion (Supplementary Figure S9), in agreement with data on Figure 2C. In XP-C cells, the photorepair of CPD significantly reduced CldU/IdU ratios from an average of 2 to 1.5, while removal of 6-4PP had no effect. Importantly, the functionality of Ad6-4phr in these cell lines was controlled by immunofluorescence performed in parallel (Supplementary Figure S7). Similar results were obtained for XP-C shRev3L. In contrast, when Polη or Rev1 was depleted in XP-C cells, the photoremoval of either 6-4PP or CPD significantly decreased replication fork stalling (Figure 6). Despite the high dose used in the DNA fiber assay, these data corroborate the effects of both 6-4PP and CPD-specific photorepair in the early S phase arrest of these cells upon low UVC doses assessed by cell cycle analysis (Figure 5).

6-4PP photorepair abolishes the generation of ssDNA gaps and postreplication repair tracts

We next investigated the involvement of 6-4PP and CPD in the generation of ssDNA gaps by evaluating, in cells transduced with photolyases: (i) the formation of ssDNA upon replication fork restart by DNA fiber assay in the presence of S1 nuclease (Figure 7A and B), and (ii) gap-filling by quantifying PRR tract density (Figure 7C and D). Because we were able to detect the presence of ssDNA on ongoing replication forks upon UV treatment in XP-C shCT (Figure 3C and D), we performed the same assay in these cells transduced with Ad6-4phr, AdCPDphr or mock-treated exposed to 50 J/m² in photorepair conditions (experimental scheme in Figure 7A, see Materials and Methods for further details). In XP-C shCT (Figure 7B), the S1 nuclease
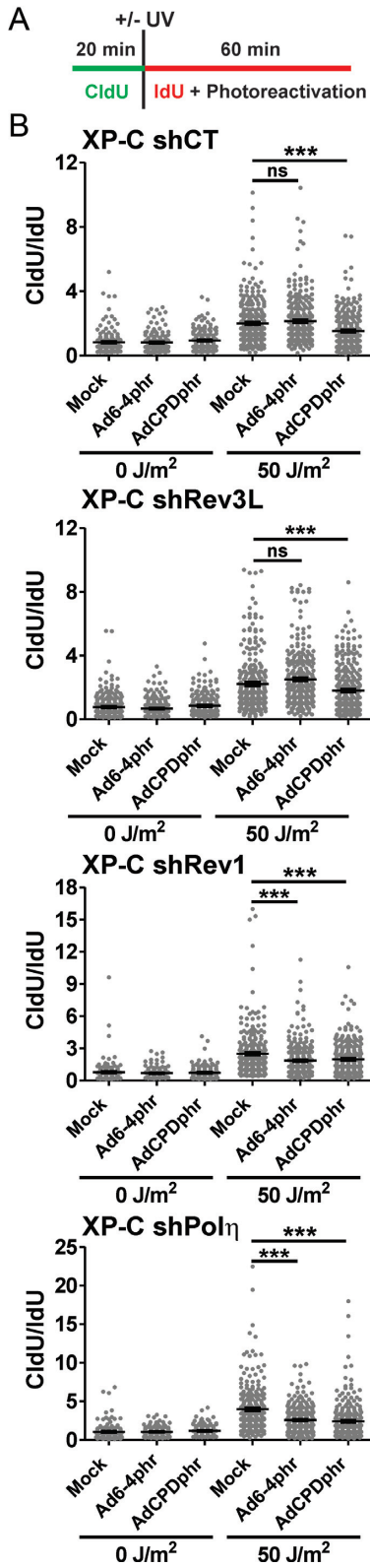
Figure 5. Effects of 6-4PP and CPD photorepair on cell cycle distribution. (**A**) Cell cycle phases of Ad6-4phr or AdCPDphr-transduced fibroblasts were evaluated by BrdU and DNA content (PI) staining 24 h after 0 or 5 J/m^2 of UVC irradiation under photorepair conditions. Representative graphics of at least two independent experiments are shown, and the percentages of cells in early S, late S and G2/M phases are indicated. At the top right of each panel, the cell cycle distribution determined only by PI staining is represented. (**B**) Quantification of cells in early S phase (left panels) and late S + G2 (late S/G2) phases (right panels) in transduced XP-C cells depleted for TLS Pols with shRNA 24 and 72 h after 2 J/m^2 and 24 h upon 5 J/m^2. Data are expressed as means of percentages (± SEM) from at least two independent experiments. The significance of differences was assessed by one-way ANOVA followed by Bonferroni test (* $P < 0.05$, ** $P < 0.01$, *** $P < 0.001$).

Figure 6. Effects of 6-4PP and CPD photoremoval on replication forks progression. (**A**) Scheme of DNA fiber assay in cells transduced with Ad-CPDphr, Ad6-4phr or mock-transduced in photorepair conditions. (**B**) CldU/IdU ratios from XP-C cells depleted for TLS Pols upon 0 or 50 J/m^2. At least 100 fibers for 0 J/m^2 and 150 for 50 J/m^2 were scored per experiment, which were performed twice independently. Statistical significances were assessed by one-way ANOVA followed by Bonferroni test (ns, non significant; ** $P < 0.01$, *** $P < 0.001$).
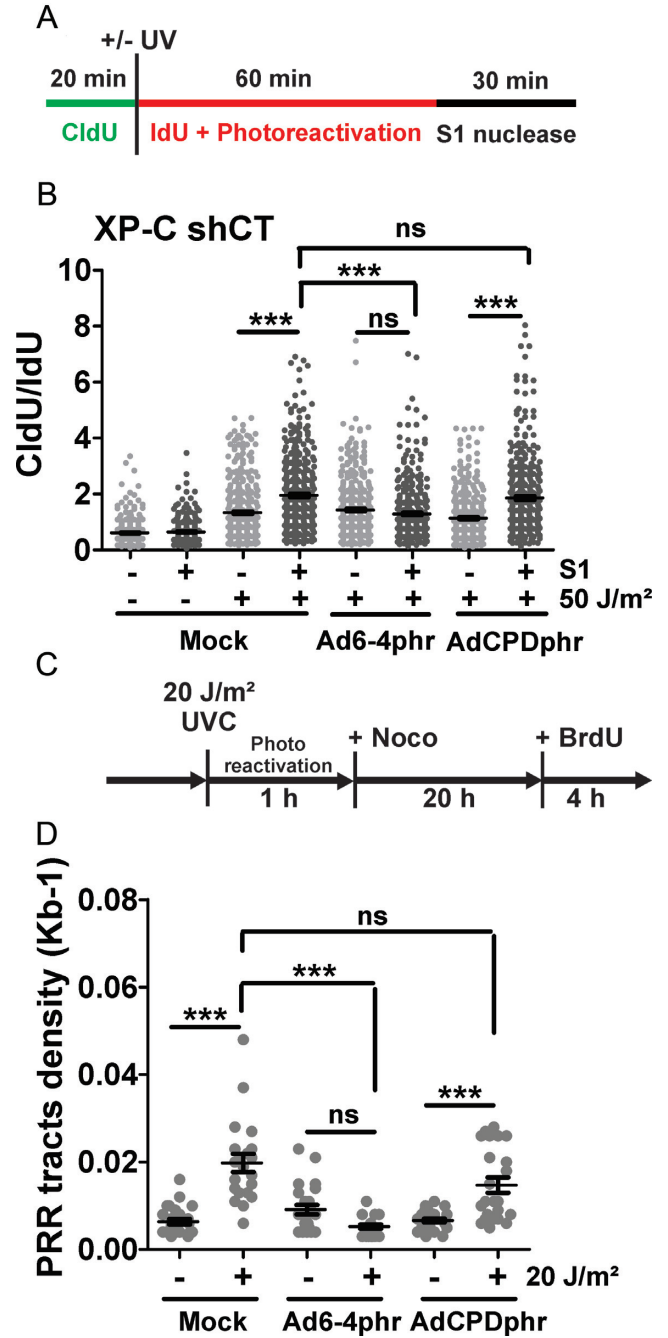
Figure 7. Effects of 6-4PP and CPD photorepair on ssDNA gaps formation and postreplication repair (PRR) tracts. XP-C shCT cells were transduced with Ad6-4phr, AdCPDphr or mock-treated. (**A**) Scheme of DNA fiber assay with the ssDNA-specific S1 nuclease in photorepair conditions. (**B**) CldU/IdU ratios from XP-C cells exposed to 0 or 50 J/m^2 and treated or not with S1 from three independent experiments ($\geq$100 fibers for 0 J/m^2 and $\geq$150 fibers for 50 J/m^2 each). (**C**) Scheme for PRR tract detection in photorepair conditions. (**D**) Quantification of PRR tracts density 24 h upon exposure to 0 or 20 J/m^2. Statistical significances were determined by one-way ANOVA followed by Bonferroni test (ns, non significant; * $P < 0.05$, *** $P < 0.001$).

increased the CldU/IdU ratio of UV-exposed cells, confirming the formation of ssDNA gaps upon 50 J/m^2. The photorepair of 6-4PP abolished the effect of S1 nuclease in cells exposed to UV, while the removal of CPD had no effect. Importantly, in the absence of S1 nuclease, the photorepair of CPD significantly decreased CldU/IdU ratio compared to mock-treated cells (Supplementary Figure S10A), in agreement with Figure 6, indicating that CPD stall forks in these cells. Since in XP-C shRev3L cells the S1 nuclease was able to increase CldU/IdU ratio from UV-exposed cells (Figure 3D), we repeated the experiment with photolyases and S1 nuclease in these cells. The results obtained were similar to those observed for XP-C shCT cells (Supplementary Figure S10B). To further confirm that 6-4PP, and not CPD, were involved in the generation of ssDNA gaps, we evaluated gap-filling in XP-C shCT cells transduced with photolyases (Figure 7C and D), and observed that when 6-4PP were removed, there was no increase in PRR tract density compared to nonirradiated cells. On the other hand, the removal of CPD induced a slightly but not statistically significant reduction on PRR tract density when compared to mock-treated XP-C cells exposed to UV. In conclusion, 6-4PP, but not CPD, are bypassed by gap-filling upon replication fork restart downstream the lesion.

DISCUSSION

In this work, we investigated the mechanisms by which UV-induced lesions are tolerated by TLS in the human genome. Tolerance of DNA damage by specialized polymerases can occur by two nonmutually exclusive mechanisms: directly at the replication forks stalled by the lesion, or behind the advancing fork to fill in ssDNA gaps generated by replication restart after the blocking damage (23,24,48). We and others have demonstrated that Polη acts at replication forks stalled at UV-induced DNA damage (24,38,42). In a similar way, herein, we observed that depletion of Rev1 in XP-C cells induces a prolonged S phase arrest of the cell cycle (Figure 2A) and a pronounced replication fork stalling, as observed by DNA fiber assay after UV exposure (Figure 2C and D). This confirms previous work showing that Rev1 knockout (KO) delays fork progression in UV-irradiated mouse embryonic fibroblasts (MEFs) (18). Therefore, the data indicate that not only Polη but also Rev1 plays a role in UV damage bypass directly at the blocked replication fork, in agreement with previous work (23). Interestingly, a recent report indicated that, in human and mouse cells, Rev1 is an indispensable scaffolding component for TLS Pols like Polη (49). On the other hand, disruption of Rev3L in XP-C cells did not increase replication fork stalling (Figure 2C and D). This lack of effect of Rev3L depletion on the progression of replication forks was also observed, by DNA fiber assays, in Rev3 KO MEFs (50) and chicken DT40 cells (51). Instead, in cells depleted for Rev3L, we detected ssDNA gaps (Figure 3) that were not repaired (Figure 4E and F) and induced a G2 phase arrest (Figure 2A). Moreover, in XP-C cells, ssDNA gaps were generated on ongoing forks in a similar manner as in XP-C shRev3L cells (Figure 3D). However, these gaps were then filled (Figure 4C, E and F), and ssDNA regions were no longer detected (Figure 3A and Supplementary Figure S4B). Therefore, we demonstrate that,

in UV-exposed human XP-C cells, ssDNA gaps arise during replication and persist into the late S/G2 phase, where they are filled in a Polζ-dependent manner. These ssDNA regions are triggers for checkpoint activation (18,44), therefore signaling for a prolonged G2 phase arrest in cells depleted for Rev3L, as shown elsewhere (19).

The involvement of Rev1 in the gap-filling pathway in higher eukaryotes is a matter of debate (18,23,28). Strikingly, Rev1 deficiency disturbed the generation of ssDNA gaps on ongoing forks 1 h after UV exposure (Figure 3E), although we were able to detect gap-filling in those cells 24 h after treatment (Figure 4E and F). These results indicate that Rev1 deficiency may impair fork restart, and back-up mechanisms allow DNA damage bypass. Interestingly, our data indicate that Rev1 is not essential for gap-filling. Altogether, our data demonstrate that in human cells, Polη and Rev1 act directly at stalled replication forks, while Polζ plays a role behind the advancing fork by filling in ssDNA gaps.

In this study, the choice of repair-deficient XP-C cells as a model allowed us to accurately study the bypass of 6-4PP besides CPD, avoiding any masking effect of the removal of these lesions by NER. By taking advantage of recombinant adenovirus carrying the cDNA coding for specific CPD or 6-4PP photolyases, we demonstrate, for the first time, that CPD, but not 6-4PP, induces prolonged blockage of replication forks in XP-C cells (Figure 6). However, 6-4PP were responsible for CAF-induced sensitivity of XP-C cells exposed to UV (Supplementary Figure S8), while in XP-V cells, CPD were the cause of the toxicity of this concomitant treatment (Supplementary Figure S8). We and others have previously demonstrated that CAF toxicity is related to the collapse of UV-induced ssDNA into DSB (24,46). Therefore, these results suggest that the persistence of unrepaired 6-4PP leads to the formation of ssDNA regions, as previously demonstrated by Jansen and colleagues (18,19). The photoremoval of 6-4PP could reduce the frequency of ssDNA regions, and therefore the generation of DSB in the presence of CAF. Indeed, 6-4PP, but not CPD, were responsible for the generation of ssDNA gaps on ongoing forks and for the gap-filling detected by PRR tracts (Figure 7). PRR tracts density was about 1 BrdU patch per 60 kb (Figure 4). Results from our group showed that 20 J/m^2 UVC irradiation generates one lesion (both CPD and 6-4PP) per 15 kb in one strand (52), what corresponds to one 6-4PP per 45–60 kb. These results further confirm that 6-4PP rather than CPD are involved in PRR tracts formation. Additionally, the photoremoval of 6-4PP, but not CPD, attenuated late S/G2 phase arrest in XP-C cells exposed to low doses of UVC (Figure 5). Therefore, unrepaired 6-4PP do not promote prolonged blockage of replication fork, but induce the formation of ssDNA gaps, ultimately triggering a late S/G2 phase arrest. Altogether, these data strongly suggest that 6-4PP, and not CPD, are the type of UV-induced damage that is tolerated through a gap-filling pathway in the human genome. Moreover, we report here that, in cells depleted for Polη or Rev1, both 6-4PP and CPD impaired S phase progression (Figure 5) and stalled replication forks (Figure 6). Therefore, we demonstrate that Polη and Rev1 are involved in the tolerance of both 6-4PP and CPD in the
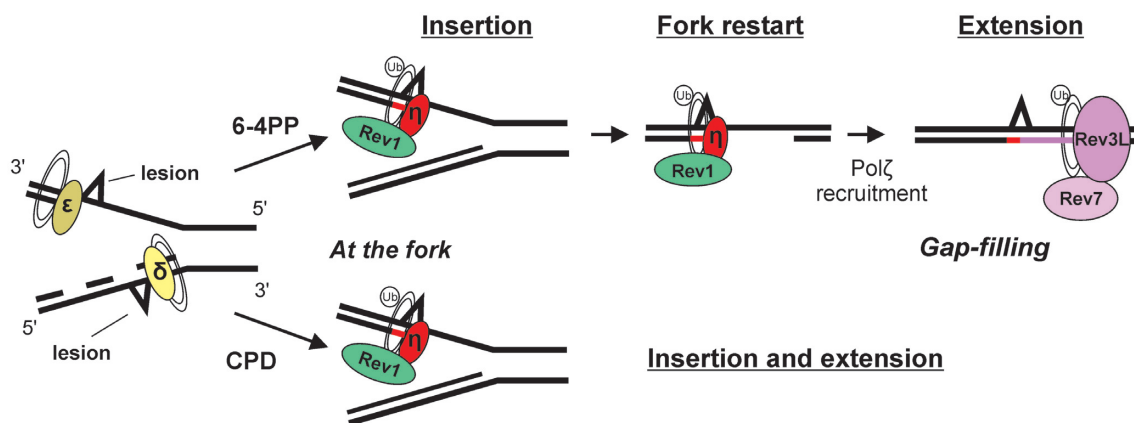
Figure 8. Model for bypass of UV-induced DNA damage, 6-4PP and CPD, in the human genome. For both CPD and 6-4PP, Rev1 and Polη perform insertion of one nucleotide opposite to the lesion at the stalled fork. Polη extends the primer and completes the bypass of CPD at the fork. In the case of 6-4PP, Polη stalls and a single-stranded DNA gap is formed upon fork restart. Gap-filling and extension are then performed by Rev3L, the catalytic subunit of Polζ, independently of the replication fork. Polζ can be recruited to DNA through interaction with Rev1, PCNA or switching with Polδ. Both pathways may occur at the leading and lagging strand. See text for more details.

human genome, and these TLS Pols play a role directly at stalled replication forks.

To summarize our findings, we propose a model for the tolerance of UV-induced 6-4PP and CPD (Figure 8). Polη and Rev1 are recruited to PCNA at replication forks stalled by either 6-4PP or CPD. Rev1 may be recruited first by interaction with PCNA (53), therefore acting as a scaffold to Polη assembly through protein–protein interaction (54), as recently proposed by Prakash's group (49). Polη performs the complete bypass of CPD (10), while it inserts one nucleotide opposite to 6-4PP (20,21) and stalls, as suggested elsewhere (55). TLS extension of 6-4PP could be performed by Polκ (56) or by Polζ (11,21) at the stalled fork since we observed that depletion of Rev3L also induces an accumulation of cells in the S phase (Figure 2A). However, our data indicate that the main role of Polζ is not at the stalled fork, but at the gap-filling pathway, and independently of S phase (Figures 2, 3 and 4). Also, we demonstrate that in the case of 6-4PP, stalled replication forks can also be restarted downstream the damage, thereby leaving ssDNA gaps behind the advancing fork (Figure 7). This restart can occur by repriming performed by Polα in both leading and lagging strand (57) and/or by the recently characterized Prim-Pol (58) in the leading strand. Additionally, replication fork restart may be mediated by new origin firing or fork convergence (59). The generated ssDNA gaps are filled by Polζ and this polymerase is essential for this pathway. Polζ can be recruited by different nonexclusive manners: interaction with Rev1 or mono-ubiquitinated PCNA (17), or by switching with Polδ (60). It has recently been proposed that TFII-I can also bridge PCNA to Polζ to promote TLS (61). Interestingly, since the gap-filling process may occur independently of fork progression, DNA synthesis by Polζ could take place with a completely different replication machinery.

The broad range of possibilities for Polζ recruitment to the DNA justifies our observation that Rev1 is not essential for gap filling. Nevertheless, an incomplete depletion of Rev1 could have led to a slower action of this protein, what

would allow a delayed gap filling by Polζ. However, the results described in this work are supported by a recent work demonstrating that, in human cells, Rev1 helps to bypass DNA damage in conjunction with Polη, Polι and Polκ, but it is totally dispensable for TLS mediated by Polζ (49).

Interestingly, it was shown that yeast Polζ is able to insert nucleotides in the bypass of 6-4PP in duplex plasmid (16), thus, we cannot exclude the possibility that both insertion and extension steps to bypass 6-4PP may be mediated by Polζ. Alternatively, redundancy of Y polymerases could explain how the insertion step takes place in the absence of Polη. Indeed, as elegantly demonstrated in Polη-deficient cells (22,62), the insertion of one nucleotide in the bypass of both CPD and 6-4PP can be performed by Polι and/or Polκ. Moreover, human Polι, besides Polη, is able to promote the insertion step in TLS of 6-4PP carried on a duplex plasmid (21). It is noteworthy that TLS at stalled forks and by gap filling may occur at both leading and lagging strands.

In conclusion, we demonstrated, with direct methodologies, that in the human genome, UV-induced gap filling is specific for 6-4PP, while bypass at stalled replication forks can occur for both 6-4PP and CPD. Moreover, we showed that while Polη and Rev1 act at arrested replication forks, Polζ is essential for gap-filling, in an S-phase-independent mechanism. Therefore, we propose that replication fork stalling at 6-4PP lesion is resolved by an insertion step at the blocked fork, followed by fork restart and gap-filling to extend the primer and conclude TLS. We are currently investigating whether in the absence of functional Polη CPD are tolerated by a similar pathway involving back-up TLS Pols. These results support the notion that the mechanism of TLS depends on the DNA polymerases involved and on the nature of DNA lesion. The findings for UV-induced photoproducts raise the question on how these mechanisms act for other types of DNA damage.

SUPPLEMENTARY DATA

Supplementary Data are available at NAR Online.

REFERENCES

1. Kaufmann,W.K. and Cleaver,J.E. (1981) Mechanisms of inhibition of DNA-replication by ultraviolet-light in normal human and xeroderma pigmentosum fibroblasts. *J. Mol. Biol.*, **149**, 171–187.
2. Cleaver,J.E. (1968) Defective repair replication of DNA in xeroderma pigmentosum. *Nature*, **218**, 652–656.
3. Menck,C.F. and Munford,V. (2014) DNA repair diseases: what do they tell us about cancer and aging? *Genet. Mol. Biol.*, **37**, 220–233.
4. Pfeifer,G. (1997) Formation and processing of UV photoproducts: effects of DNA sequence and chromatin environment. *Photochem. Photobiol.*, **65**, 270–283.
5. Mitchell,D.L. (1988) The induction and repair of lesions produced by the photolysis of (6-4) photoproducts in normal and UV-hypersensitive human cells. *Mutat Res*, **194**, 227–237.
6. Costa,R., Chigançans,V., Galhardo,R.S., Carvalho,H. and Menck,C. (2003) The eukaryotic nucleotide excision repair pathway. *Biochimie*, **85**, 1083–1099.
7. Riou,L., Zeng,L., Chevallier-Lagente,O., Stary,A., Nikaido,O., Taïeb,A., Weeda,G., Mezzina,M. and Sarasin,A. (1999) The relative expression of mutated XPB genes results in xeroderma pigmentosum/Cockayne's syndrome or trichothiodystrophy cellular phenotypes. *Hum Mol Genet*, **8**, 1125–1133.
8. Sale,J.E. (2012) Competition, collaboration and coordination–determining how cells bypass DNA damage. *J Cell Sci*, **125**, 1633–1643.
9. Lange,S.S., Takata,K. and Wood,R.D. (2011) DNA polymerases and cancer. *Nat Rev Cancer*, **11**, 96–110.
10. Masutani,C., Kusumoto,R., Yamada,A., Dohmae,N., Yokoi,M., Yuasa,M., Araki,M., Iwai,S., Takio,K. and Hanaoka,F. (1999) The XPV (xeroderma pigmentosum variant) gene encodes human DNA polymerase eta. *Nature*, **399**, 700–704.
11. Guo,D., Wu,X., Rajpal,D.K., Taylor,J.S. and Wang,Z. (2001) Translesion synthesis by yeast DNA polymerase zeta from templates containing lesions of ultraviolet radiation and acetylaminofluorene. *Nucleic Acids Res*, **29**, 2875–2883.
12. Shachar,S., Ziv,O., Avkin,S., Adar,S., Wittschieben,J., Reissner,T., Chaney,S., Friedberg,E.C., Wang,Z., Carell,T. *et al.* (2009) Two-polymerase mechanisms dictate error-free and error-prone translesion DNA synthesis in mammals. *EMBO J*, **28**, 383–393.
13. Livneh,Z., Ziv,O. and Shachar,S. (2010) Multiple two-polymerase mechanisms in mammalian translesion DNA synthesis. *Cell Cycle*, **9**, 729–735.
14. de Groote,F.H., Jansen,J.G., Masuda,Y., Shah,D.M., Kamiya,K., de Wind,N. and Siegal,G. (2011) The Rev1 translesion synthesis polymerase has multiple distinct DNA binding modes. *DNA Repair*, **10**, 915–925.
15. Sharma,N.M., Kochenova,O.V. and Shcherbakova,P.V. (2011) The non-canonical protein binding site at the monomer-monomer interface of yeast proliferating cell nuclear antigen (PCNA) regulates the Rev1-PCNA interaction and Polζ/Rev1-dependent translesion DNA synthesis. *J Biol Chem*, **286**, 33557–33566.
16. Gibbs,P.E., McDonald,J., Woodgate,R. and Lawrence,C.W. (2005) The relative roles in vivo of Saccharomyces cerevisiae Pol eta, Pol zeta, Rev1 protein and Pol32 in the bypass and mutation induction of an abasic site, T-T (6-4) photoadduct and T-T cis-syn cyclobutane dimer. *Genetics*, **169**, 575–582.
17. Szüts,D., Marcus,A.P., Himoto,M., Iwai,S. and Sale,J.E. (2008) REV1 restrains DNA polymerase zeta to ensure frame fidelity during translesion synthesis of UV photoproducts in vivo. *Nucleic Acids Res*, **36**, 6767–6780.
18. Jansen,J.G., Tsaalbi-Shtylik,A., Hendriks,G., Gali,H., Hendel,A., Johansson,F., Erixon,K., Livneh,Z., Mullenders,L.H., Haracska,L. *et al.* (2009) Separate domains of Rev1 mediate two modes of DNA damage bypass in mammalian cells. *Mol Cell Biol*, **29**, 3113–3123.
19. Temviriyanukul,P., van Hees-Stuivenberg,S., Delbos,F., Jacobs,H., de Wind,N. and Jansen,J.G. (2012) Temporally distinct translesion synthesis pathways for ultraviolet light-induced photoproducts in the mammalian genome. *DNA Repair (Amst)*, **11**, 550–558.
20. Bresson,A. and Fuchs,R.P. (2002) Lesion bypass in yeast cells: Pol eta participates in a multi-DNA polymerase process. *EMBO J*, **21**, 3881–3887.
21. Yoon,J.H., Prakash,L. and Prakash,S. (2010) Error-free replicative bypass of (6-4) photoproducts by DNA polymerase zeta in mouse and human cells. *Genes Dev*, **24**, 123–128.
22. Jansen,J.G., Temviriyanukul,P., Wit,N., Delbos,F., Reynaud,C.A., Jacobs,H. and de Wind,N. (2014) Redundancy of mammalian Y family DNA polymerases in cellular responses to genomic DNA lesions induced by ultraviolet light. *Nucleic Acids Res*, **42**, 11071–11082.
23. Edmunds,C.E., Simpson,L.J. and Sale,J.E. (2008) PCNA ubiquitination and REV1 define temporally distinct mechanisms for controlling translesion synthesis in the avian cell line DT40. *Mol Cell*, **30**, 519–529.
24. Quinet,A., Vessoni,A.T., Rocha,C.R.R., Gottifredi,V., Biard,D., Sarasin,A., Menck,C.F.M. and Stary,A. (2014) Gap-filling and bypass at the replication fork are both active mechanisms for tolerance of low-dose ultraviolet-induced DNA damage in the human genome. *DNA Repair*, **14**, 27–38.
25. Meneghini,R. (1976) Gaps in DNA synthesized by ultraviolet light-irradiated WI38 human cells. *Biochim Biophys Acta*, **425**, 419–427.
26. Lopes,M., Foiani,M. and Sogo,J.M. (2006) Multiple mechanisms control chromosome integrity after replication fork uncoupling and restart at irreparable UV lesions. *Mol Cell*, **21**, 15–27.
27. Daigaku,Y., Davies,A.A. and Ulrich,H.D. (2010) Ubiquitin-dependent DNA damage bypass is separable from genome replication. *Nature*, **465**, 951–U913.
28. Diamant,N., Hendel,A., Vered,I., Carell,T., Reissner,T., de Wind,N., Geacinov,N. and Livneh,Z. (2012) DNA damage bypass operates in the S and G2 phases of the cell cycle and exhibits differential mutagenicity. *Nucleic Acids Res*, **40**, 170–180.
29. Menck,C. (2002) Shining a light on photolyases. *Nat Genet*, **32**, 338–339.
30. Moraes,M.C., de Andrade,A.Q., Carvalho,H., Guecheva,T., Agnoletto,M.H., Henriques,J.A., Sarasin,A., Stary,A., Saffi,J. and Menck,C.F. (2012) Both XPA and DNA polymerase eta are necessary for the repair of doxorubicin-induced DNA lesions. *Cancer Lett*, **314**, 108–118.
31. Gomes,L.R., Vessoni,A.T. and Menck,C.F. (2015) Three-dimensional microenvironment confers enhanced sensitivity to doxorubicin by reducing p53-dependent induction of autophagy. *Oncogene*, **34**, 5329–5340.
32. Bhat,A., Andersen,P.L., Qin,Z. and Xiao,W. (2013) Rev3, the catalytic subunit of Polζ, is required for maintaining fragile site stability in human cells. *Nucleic Acids Res*, **41**, 2328–2339.
33. Shim,H.S., Wei,M., Brandhorst,S. and Longo,V.D. (2015) Starvation promotes REV1 SUMOylation and p53-dependent sensitization of melanoma and breast cancer cells. *Cancer Res*, **75**, 1056–1067.
34. Cortat,B., Garcia,C.C., Quinet,A., Schuch,A.P., de Lima-Bessa,K.M. and Menck,C.F. (2013) The relative roles of DNA damage induced by UVA irradiation in human cells. *Photochem Photobiol Sci*, **12**, 1483–1495.
35. Vogt,V.M. (1973) Purification and further properties of single-strand-specific nuclease from Aspergillus oryzae. *Eur J Biochem*, **33**, 192–200.
36. Schumacher,R.I., Menck,C.F. and Meneghini,R. (1983) Sites sensitive to S1 nuclease and discontinuities in DNA nascent strands of ultraviolet irradiated mouse cells. *Photochem Photobiol*, **37**, 605–610.
37. Arlett,C.F., Harcourt,S.A. and Broughton,B.C. (1975) The influence of caffeine on cell survival in excision-proficient and excision-deficient xeroderma pigmentosum and normal human cell strains following ultraviolet-light irradiation. *Mutat Res*, **33**, 341–346.

38. Despras,E., Daboussi,F., Hyrien,O., Marheineke,K. and Kannouche,P.L. (2010) ATR/Chk1 pathway is essential for resumption of DNA synthesis and cell survival in UV-irradiated XP variant cells. *Hum Mol Genet*, **19**, 1690–1701.

39. Kaufmann,W.K., Heffernan,T.P., Beaulieu,L.M., Doherty,S., Frank,A.R., Zhou,Y., Bryant,M.F., Zhou,T., Luche,D.D., Nikolaishvili-Feinberg,N. *et al.* (2003) Caffeine and human DNA metabolism: the magic and the mystery. *Mutat Res*, **532**, 85–102.

40. Berra,C.M., de Oliveira,C.S., Garcia,C.C., Rocha,C.R., Lerner,L.K., Lima,L.C., Baptista a.,M. S. and Menck,C.F. (2013) Nucleotide excision repair activity on DNA damage induced by photoactivated methylene blue. *Free Radic Biol Med*, **61**, 343–356.

41. Andrade-Lima,L.C., Andrade,L.N. and Menck,C.F. (2015) ATR suppresses apoptosis after UVB irradiation by controlling both translesion synthesis and alternative tolerance pathways. *J Cell Sci*, **128**, 150–159.

42. Vallerga,M.B., Mansilla,S.F., Federico,M.B., Bertolin,A.P. and Gottifredi,V. (2015) Rad51 recombinase prevents Mre11 nuclease-dependent degradation and excessive PrimPol-mediated elongation of nascent DNA after UV irradiation. *Proc Natl Acad Sci U S A*, **112**, E6624–E6633.

43. Yang,Y., Liu,Z., Wang,F., Temviriyanukul,P., Ma,X., Tu,Y., Lv,L., Lin,Y.F., Huang,M., Zhang,T. *et al.* (2015) FANCD2 and REV1 cooperate in the protection of nascent DNA strands in response to replication stress. *Nucleic Acids Res.*, **43**, 8325–8339.

44. Callegari,A.J., Clark,E., Pneuman,A. and Kelly,T.J. (2010) Postreplication gaps at UV lesions are signals for checkpoint activation. *Proc Natl Acad Sci U S A*, **107**, 8219–8224.

45. Elvers,I., Johansson,F., Groth,P., Erixon,K. and Helleday,T. (2011) UV stalled replication forks restart by re-priming in human fibroblasts. *Nucleic Acids Res*, **39**, 7049–7057.

46. Elvers,I., Hagenkort,A., Johansson,F., Djureinovic,T., Lagerqvist,A., Schultz,N., Stoimenov,I., Erixon,K. and Helleday,T. (2012) CHK1 activity is required for continuous replication fork elongation but not stabilization of post-replicative gaps after UV irradiation. *Nucleic Acids Res*, **40**, 8440–8448.

47. de Lima-Bessa,K.M., Armelini,M.G., Chiganças,V., Jacysyn,J.F., Amarante-Mendes,G.P., Sarasin,A. and Menck,C.F. (2008) CPDs and 6-4PPs play different roles in UV-induced cell death in normal and NER-deficient human cells. *DNA Repair (Amst)*, **7**, 303–312.

48. Lehmann,A.R. and Fuchs,R.P. (2006) Gaps and forks in DNA replication: rediscovering old models. *DNA Repair (Amst)*, **5**, 1495–1498.

49. Yoon,J.H., Park,J., Conde,J., Wakamiya,M., Prakash,L. and Prakash,S. (2015) Rev1 promotes replication through UV lesions in conjunction with DNA polymerases η, ι, and κ but not DNA polymerase ζ. *Genes Dev*, **29**, 2588–2602.

50. Jansen,J.G., Tsaalbi-Shtylik,A., Hendriks,G., Verspuy,J., Gali,H., Haracska,L. and de Wind,N. (2009) Mammalian polymerase zeta is essential for Postreplication repair of UV-induced DNA lesions. *DNA Repair*, **8**, 1444–1451.

51. Hirota,K., Yoshikiyo,K., Guilbaud,G., Tsurimoto,T., Murai,J., Tsuda,M., Phillips,L.G., Narita,T., Nishihara,K., Kobayashi,K. *et al.* (2015) The POLD3 subunit of DNA polymerase δ can promote translesion synthesis independently of DNA polymerase ζ. *Nucleic Acids Res.*, **43**, 1671–1683.

52. Andrade-Lima,L.C., Veloso,A., Paulsen,M.T., Menck,C.F. and Ljungman,M. (2015) DNA repair and recovery of RNA synthesis following exposure to ultraviolet light are delayed in long genes. *Nucleic Acids Res*, **43**, 2744–2756.

53. Hendel,A., Krijger,P.H., Diamant,N., Goren,Z., Langerak,P., Kim,J., Reissner,T., Lee,K.Y., Geacintov,N.E., Carell,T. *et al.* (2011) PCNA ubiquitination is important, but not essential for translesion DNA synthesis in mammalian cells. *PLoS Genet*, **7**, e1002262.

54. Pustovalova,Y., Bezsonova,I. and Korzhnev,D.M. (2012) The C-terminal domain of human Rev1 contains independent binding sites for DNA polymerase η and Rev7 subunit of polymerase ζ. *FEBS Lett*, **586**, 3051–3056.

55. Jansen,J.G., Fousteri,M.I. and de Wind,N. (2007) Send in the clamps: control of DNA translesion synthesis in eukaryotes. *Mol Cell*, **28**, 522–529.

56. Haracska,L., Prakash,L. and Prakash,S. (2002) Role of human DNA polymerase kappa as an extender in translesion synthesis. *Proc Natl Acad Sci U S A*, **99**, 16000–16005.

57. Lue,N.F., Chan,J., Wright,W.E. and Hurwitz,J. (2014) The CDC13-STN1-TEN1 complex stimulates Pol α activity by promoting RNA priming and primase-to-polymerase switch. *Nat Commun*, **5**, 5762.

58. García-Gómez,S., Reyes,A., Martínez-Jiménez,M.I., Chocrón,E.S., Mourón,S., Terrados,G., Powell,C., Salido,E., Méndez,J., Holt,I.J. *et al.* (2013) PrimPol, an archaic primase/polymerase operating in human cells. *Mol Cell*, **52**, 541–553.

59. Helleday,T. (2013) PrimPol breaks replication barriers. *Nat Struct Mol Biol*, **20**, 1348–1350.

60. Baranovskiy,A.G., Lada,A.G., Siebler,H.M., Zhang,Y., Pavlov,Y.I. and Tahirov,T.H. (2012) DNA polymerase δ and ζ switch by sharing accessory subunits of DNA polymerase δ. *J Biol Chem*, **287**, 17281–17287.

61. Fattah,F.J., Hara,K., Fattah,K.R., Yang,C., Wu,N., Warrington,R., Chen,D.J., Zhou,P., Boothman,D.A. and Yu,H. (2014) The transcription factor TFII-I promotes DNA translesion synthesis and genomic stability. *PLoS Genet*, **10**, e1004419.

62. Ziv,O., Geacintov,N., Nakajima,S., Yasui,A. and Livneh,Z. (2009) DNA polymerase zeta cooperates with polymerases kappa and iota in translesion DNA synthesis across pyrimidine photodimers in cells from XPV patients. *Proc Natl Acad Sci U S A*, **106**, 11552–11557.